의학박사 학위논문

펜드린-결핍 마우스 모델에서 외반고리관의 해부학적 및 기능적 이상에 대한 연구

Anatomical and Functional Abnormalities of the Lateral Semicircular Canals in a Pendrin-Deficient Mouse Model

2016 년 8 월

서울대학교 대학원

의학과 이비인후과학 전공

안 용 휘

펜드린-결핍 마우스 모델에서 외반고리관의 해부학적 및 기능적 이상에 대한 연구

지도교수 이 준 호

이 논문을 의학과 박사 학위논문으로 제출함

2016 년 4 월

서울대학교 대학원

의학과 이비인후과학전공

안 용 휘

안용휘의 박사 학위논문을 인준함

2016 년 7 월

위원장 오 승 하 (인)

부위원장 이 준 호 (인)

위원 조 양 선 (인)

위원 김 성 준 (인)

위원 최 병 윤 (인)

Anatomical and Functional Abnormalities of the Lateral Semicircular Canals in a Pendrin-Deficient Mouse Model

by

Yong-Hwi An

A Thesis Submitted to the Department of Otolaryngology in Fulfillment of the Requirements for the Degree of Doctor of Philosophy in Medicine

at the Seoul National University College of Medicine

July, 2016

Approved by thesis committee

Chairman	Seung Ha Oh
Vice chairman	Jun Ho Lee
Member	Yang-Sun Cho
Member	Sung Joon Kim
Member	Byung Yoon Choi

Abstract

Anatomical and Functional Abnormalities of the Lateral Semicircular Canals in a Pendrin-Deficient Mouse Model

Yong-Hwi An

Department of Otorhinolaryngology

The Graduate School

Seoul National University

Pendrin, encoded by the *SLC26A4* gene, is an anion exchanger protein expressed in the epithelial cells of inner ear. Clinically, the absence of pendrin results in hearing loss associated with enlarged vestibular aqueduct; it is simultaneously observed with dizziness and postural imbalance. The aim of this study was to investigate the quantitative responses of vestibulo-ocular reflex (VOR) and anatomical abnormalities of the lateral semicircular canal (LSC) in a pendrin-deficient mice strain. The mice strain consisted of wild type mice and three distinct genetic conditions: homozygous knockout mice, transgenic mice with doxycycline-

inducible expression of *Slc26a4*, and heterozygotes. Hearing and balancing systems were evaluated by auditory brainstem response, sinusoidal harmonic acceleration test, and histology of the LSC. All *Slc26a4* homozygous knockout mice showed total deafness, whereas the remaining strains had normal hearing, indicating all-or-none phenotype of auditory function. The sinusoidal harmonic acceleration test exhibited minimal VOR responses in homozygotes and intermediate responses in transgenic mice and heterozygotes compared with normal controls. This outcome implies a pendrin dose-dependent pattern of vestibular dysfunction. Vacuolar replacement and absence of calretinin expression of vestibular hair cells in the LSC were identified in homozygotes. However, no apparent difference in inner ear architectures among wild-type, heterozygous, and transgenic mice were identified. These results suggest that mutations of *Slc26a4* gene in mouse models induce diverse functional deficits of the LSC and vestibular diseases with variable manifestations.

Keywords: Pendrin, *SLC26A4*, vestibule-ocular reflex, lateral semicircular canal, vestibular diseases, enlarged vestibular aqueduct, sensorineural hearing loss

Student Number: 2010-30525

목차

List of Figures

List of Abbreviations and Symbols

Vestibulo-ocular reflex (VOR)

Lateral semicircular canal (LSC)

Enlarged vestibular aqueduct (EVA)

Mice with unilateral labyrinthectomy (ULx)

Slc26a4 homozygous knockout mice (*Slc26a4*$^{\Delta/\Delta}$)

Transgenic mice with doxycycline-inducible expression of *Slc26a4*

(Tg(+);*Slc26a4*$^{\Delta/\Delta}$)

Slc26a4 heterozygous knockout mice (*Slc26a4*$^{\Delta/+}$)

Wild type mice for *Slc26a4* (*Slc26a4*$^{+/+}$)

Decibel (dB)

Hertz (Hz)

Degree (°)

Second (s)

Minute (min)

Hour (h)

INTRODUCTION

Pendrin is a member of the *SLC26A4* family of Cl^--dependent anion transporters that are predominantly expressed at the apical membrane of many epithelia. Pendrin-mediated reaction occurs by the electro-neutral exchange of Cl^- for HCO_3^- (Royaux et al., 2001; Soleimani et al., 2001), iodide (I^-) (Dossena et al., 2006; Scott et al., 1999), or thiocyanate (SCN^-) (Pedemonte et al., 2007). Pendrin functions as a mediator between Cl^- and HCO_3^- in the mouse inner ear (Wangemann et al., 2007). Furthermore, pendrin functions in the secretion of HCO_3^- into endolymph functions as an essential process to maintain pH and ionic homeostasis in both cochlea which administers the auditory portion of the inner ear, and vestibule responsible for the system of balance and equilibrium.

Mutations in *SLC26A4* cause a broad phenotypic spectrum of cochlear and vestibular dysfunctions from a typical Pendred syndrome to a non-syndromic enlarged vestibular aqueduct (EVA). Regarding ears with EVA, there does not appear to be a relation between the presence of a cochlear anomaly and severity of hearing disturbance when other covariates such as genotype are considered (King et al., 2010). Individuals diagnosed with EVA with two *SLC26A4* mutant alleles have more significant hearing deficit than the individuals with a single or no mutant *SLC26A4* allele. This understanding indicates that the malfunctioning of pendrin contributes to the development of hearing loss in EVA, while gross morphogenetic anomalies do not. A few clinical trials on the vestibular symptoms of pendrin-

deficient humans show the incidence of disequilibrium or vertigo attacks ranging from 45% to 71%; *SLC26A4* homozygotes had more episodes of dizziness than heterozygotes (Miyagawa et al., 2014; Sugiura et al., 2005; Zalewski et al., 2015). Only one study produced objective results of vestibular function test in two patients genetically tested for *SLC26A4* mutations; each presented absence of unilateral caloric response and bilateral vestibular hypofunction (Stinckens et al., 2001). Some of the inherent difficulties in demonstrating pendrin-insufficiency vestibular phenotypes lie in the assessment of pediatric populations and the central compensation during their growth period. However, it is reported that there is no correlation between vestibular dysfunction and the number of *SLC26A4* mutant alleles, the severity of hearing disturbance, or the size of EVA anomaly (Zalewski et al., 2015). Therefore, the pathologic mechanism leading to disorders of the human balance system might differ from that of auditory dysfunction in patients with *SLC26A4* mutations.

Slc26a4 homozygous knockout mice (*Slc26a4*$^{\Delta/\Delta}$) have vestibular dysfunction, profound hearing loss, and massively enlarged endolymphatic spaces throughout the entire inner ear (Everett et al., 2001). Early-onset profound deafness and inner ear malformation in the *Slc26a4*$^{\Delta/\Delta}$ mouse model cannot possibly represent the less severe phenotypes and manifestations frequently observed in human patients with *SLC26A4* mutation (Griffith et al., 1996; King et al., 2010). Thus, transgenic mice with doxycycline-inducible expression of *Slc26a4* (Tg(+);*Slc26a4*$^{\Delta/\Delta}$) were generated to define the temporal requirements for pendrin in the inner ear and to

model human phenotypes (Choi et al., 2011; Ito et al., 2014). Administration of doxycycline initially enables *Slc26a4*-null mice to express pendrin at the exact locations of the cochlea and the vestibule; the doxycycline cessation leads to the rapid withdrawal of pendrin expression. Normal hearing was achieved by the presence of pendrin during the critical period of the inner ear development, though normal endocochlear potential was not acquired in this transgenic mouse line. *Slc26a4* heterozygous knockout mice (*Slc26a4*$^{\Delta/+}$) had normal hearing thresholds and normal latencies to fall from the rotarod test (Everett et al., 2001), suggesting an intact overall auditory and balance systems. Considering the autosomal recessive inheritance of *SLC26A4* gene, it is natural that heterozygotes are theoretically identical to the wild type mice. When compared with the detailed auditory phenotype characterization in these *Slc26a4* mutant mice, details of the vestibular phenotype, including semicircular canals anatomy and quantitative vestibulo-ocular reflex (VOR) have not been reported. So, the aim of this investigation was to evaluate the VOR responses and anatomical abnormality of the lateral semicircular canal (LSC) in pendrin-deficient mice strain.

METHODS

Animals

Pendrin-deficient mice were bred at Seoul National University Bundang Hospital in Seongnam. The generation of wild type mice (*Slc26a4*$^{+/+}$), *Slc26a4* heterozygous knockout mice (*Slc26a4*$^{\Delta/+}$), transgenic mice with doxycycline-inducible *Slc26a4* expression (Tg(+);*Slc26a4*$^{\Delta/\Delta}$), and *Slc26a4* homozygous knockout mice (*Slc26a4*$^{\Delta/\Delta}$) were previously described (Choi et al., 2011; Kim and Wangemann, 2011; Wangemann et al., 2007). In brief, the genetic background of each initially included C57BL/6J derived from *Slc26a4*$^{\Delta/\Delta}$ mice segregating a targeted deletion allele (Everett et al., 2001). To induce the expression of pendrin in Tg(+);*Slc26a4*$^{\Delta/\Delta}$, drinking water containing 0.2 g of doxycycline hyclate (Sigma-Aldrich, Sanit Louis, MO, USA) and 5 g of sucrose (MP Biomedicals, Solon, OH, USA) per 100 mL of reagent-grade water was administrated to mice (Choi et al., 2011). Doxycycline-containing water was provided to the dam from the onset of mating and substituted by doxycycline-free water at embryonic day 17.5, which was estimated from the day at which a vaginal plug was observed. All possible steps were taken to avoid animals from suffering, as well as keeping to a minimum the number of animals used in the study. Total 51 mice of 8–12 weeks, specifically *Slc26a4*$^{+/+}$ (n=9), *Slc26a4*$^{\Delta/+}$ (n=12), and Tg (+);*Slc26a4*$^{\Delta/\Delta}$ (n=13), *Slc26a4*$^{\Delta/\Delta}$ (n=8), and wild type mice with right-side unilateral labyrinthectomy (n=9), were used. Labyrinthectomy was performed as follows: A 1-cm incision was made

vertically along the posterior sulcus of the auricle of anesthetized mice lying in a prone position, and the superior and horizontal semicircular canals were exposed. Each semicircular canal was destroyed using a dental drill (Marathon-3, Saeyang Microtech, Daegu, Korea) with round burr (Cat # 342-047, round bur, 0.3 mm, Dentsply MailleferTM, Ballaiques, Switzerland). The location of leakage of the endo-perilymph and perilymph was identified, and the openings of the semicircular canals were extended toward the ampulla. Finally, the lateral wall of the vestibule was completely opened, and the endolymph was completely removed by vacuum. To maintain the open area of the vestibule, it was filled with collagen (Helitene; Intergra Life Sciences Co., Plainsboro, NJ, USA) and then muscles and skin were sutured. To confirm the effect of unilateral labrynthectomy, the tail-hanging test was performed immediately after recovery from anesthesia, as previously described (Aleisa et al., 2007). In addition, the skew deviation of the eyeball, rolling of the body toward the damaged side, and head tilting to the damaged side were checked. All of the experiments and procedures were approved by the Institutional Animal Care and Use Committee at Seoul National University Bundang Hospital.

Auditory evaluation

Mice were anesthetized by isoflurane gas inhalation (Aerane, O_2 5L/min, 2.0, Ilsung Pharm.co, Seoul, Korea). TDT System-3 (Tucker Davies Technologies, Gainseville, FL, USA) was used to measure the thresholds of the mice auditory brainstem response. Click sounds at varying intensity (10–120 dB SPL) were given

to evoke auditory brainstem response of the mice. Supra-threshold stimulus intensities were initially decreased in 10-dB steps, followed by 5-dB steps at lower intensities to determine the response threshold. Mice were kept on a heating pad in a sound-proof chamber during testing (Modular anechoic booth, SONTEK, Pa-Ju, Gyeonggi, Korea).

Vestibular functional evaluation

For checking VOR, sinusoidal harmonic acceleration test was performed as demonstrated previously (Kim et al., 2012). Before recording the nystagmus, flat head screw (Stainless Sara Piece M2x16 mm, Hyun Jin Precision Co. Ltd., Pa-Ju, Gyeonggi, Korea) was temporarily implanted on the place between bregma and lambda by OptiBond prime (Kerr, CA), OptiBond adhesive (Kerr, CA), and Charisma composite (Heraeus Kulzer, Germany) with 1-min curing (Maxima 480 visible light curing unit; Henry Schein Inc., Melville, NY, USA) (de Jeu et al., 2012). Then, the upper and lower eyelids were sutured in an everting manner (D-7308M2, Deknatel; Teleflex Medical, Research Triangle Park, NC, USA) to prevent blinking and ensure maximal eyeball exposure. All the above procedures were accomplished with body temperature kept at 37°C by heating pad. Before recovering from anesthesia, the mouse was placed in a prone position in a Broome style restrainer made in-house to limit body movements. The mouse's head was completely fixed to a sinusoidal rotational stimulator (M-YS4080FN001, NSK, Ukiha-shi, Fukuoka, Japan) by inserting the previous implanted screw into the head

fixation structure (Hyunjin precision, Seoul, Korea). The restrainer and tail were also taped onto the machine to prevent further movement. The camera (FL3-U3-13Y3M-C; Point Grey Research Inc., Richmond, BC, Canada) was focused by adjusting the micro-stage (ST-SW-60, SS3V-25L, Science town Co., Incheon, Korea). The marker was designed using Adobe Illustrator CS4, v14.00 (Adobe Systems Inc., Mountain View, California, USA) as an isosceles triangle, with a length of 400 μm for the two equal sides and then printed on royal art papers (C1S-75, Ballarpur industries Limited, Haryana, India) using an inkjet printer (Hewlett-Packard®, Palo Alto, CA, USA). Subsequently, proparacaine hydrochloride (Alkain 5% ophthalmic solution, S. A. Alcon-Couvreur N.V, Purrs, Belgium) was applied to the mouse's eye, followed by the attachment of the prepared marker to the pupil using a cyanoacrylate (Histoacryl®, Tissueseal, Ann Arbor, MI, USA). An ointment (terramycin eye ointment®, Pfizer Inc. Seoul, Korea) was applied to the other eye to prevent visual fixation.

All incidences of nystagmus were recorded at 120 fps in a dark room under 10 lux using a telecentric lens (TCL1.0x-40-ST, SPO Inc., Daejeon, South Korea) and 6 extension tubes (ML-EXR5; Point Grey Research Inc.). The recorded images were processed with the digital-video-based tracking system using the image subtraction technique. LabVIEW (National Instruments, Austin, Texas, USA) was used to simultaneously monitor horizontal nystagmus. The VOR frequency response was characterized during earth vertical rotation at 0.1, 0.2, and 0.5 Hz with a peak velocity of 60 and 100°/s.

Nystagmus analysis was based on a comparison of the stimulation and response. Here the head (°/s) and slow phase eye velocity of nystagmus (°/s) served as stimulation and response, respectively. A minimum of three cycles were summated on a one-cycle-scaled chart to calculate the average of the three cycles. Then, the average slow phase sine curve was compared to the head velocity sine curve to calculate gain.

Histology and immunohistochemistry of the LSC

Mice were euthanized by CO_2 exposure and decapitation was performed following the Institutional Animal Care and Use Committee protocol. The inner ears were dissected from the temporal bones and processed as previously described (Noben-Trauth et al, 2010) using the ImmunoBed Kit (Polysciences Inc.) and a Leica RM2265 microtome. Sections of 5-µm thickness were stained with 1% toluidine blue. Images were captured with ACT-1 software and a Nikon Digital Cam DXM1200 attached to a Nikon Eclipse 90i light microscope. Anti-pendrin antisera were generated by immunizing rabbits (Covance) with a synthetic peptide (NH2-CEELDVQDEAMRRLAS; Princeton BioMolecules) that had a non-coding amino-terminal cysteine for linking to an affinity matrix and to 766–780 amino acids of the mouse pendrin C-terminus (NCBI NP_035997). Three rabbits were immunized to generate PB824, PB825, and PB826 antisera. Anti-pendrin IgG was purified with immobilized protein A (Pierce) followed by affinity column purification using an AminoLink Plus Immobilization Kit (Pierce). Specimens were stained with

hematoxylin and eosin, and morphology of each sample was examined on a Leica optical microscope. Pre-absorption and Western blot evaluations of polyclonal rabbit anticalretinin (Millipore, Bedford, MA; AB5054) antibodies were used (Baizer and Broussard, 2010) to determine their specificity for calretinin which is mainly expressed from the type I vestibular hair cells of the inner ear. Before the application of antibodies, specimens were incubated with 5% normal goat serum for 1 h at room temperature. Specimens were incubated with primary antibodies of 1:250 dilution anti-calretinin for 2 h at room temperature. After washing three times with phosphate buffered saline, secondary antibodies of Alexa Fluor 488 were conjugated to goat anti-rabbit (Invitrogen) at 1:100 for 30 min at room temperature. At the end of all the staining steps, the preparations were washed with buffered saline and mounted in DAPI (4',6-diamidino-2-phenylindole) medium (Vector). Whole-mounted mouse ampullae of the LSC were immunostained essentially as described for pendrin (Choi et al., 2011) with sections were 10-μm thick, and the blocking solution was PBS with 2% bovine serum albumin and 5% normal goat serum. Primary antibodies were diluted 1:1000 (PB826) in blocking solution, and the secondary antibody was Alexa Fluor 488–conjugated goat anti-rabbit IgG (#A-11008; Invitrogen) diluted 1:500. Tissues were counterstained with rhodamine-phalloidin (Molecular Probes) at a 1:100 dilution. Slides were mounted with ProLong Gold antifade reagent (Invitrogen). Images were captured with an LSM780 confocal microscope.

Measurement of endolymphatic potential in the LSC ampulla

Adult mice (P60-P90) were anesthetized with 4% tribromoethanol (13μl/g body weight i.p.). Glass electrodes were manufactured from filament-containing glass tubing (1B100F-4 World Precision Instruments, Sarasota, FL, USA) using a micropipette puller (Narishige PE-22, Tokyo, Japan). The electrodes were filled with 1M KCl solution. The enolymphatic potential in the LSC ampulla was measured using the electrode. Measurements were made in the LSC ampulla via ventral approach of the mice. After exposing the bulla, the bony shell of bulla, part of tympanic membrane, and ossicles (malleus and incus) were removed, and the LSC ampulla was identified at the inferolateral side of oval window. A small bony hole was made with a 30 gauge needle at the ampullary area and the electrode was advanced through the hole. Data were recorded digital for data analysis (DIGIDATA 1440A and Axoscope 10, Axon Instruments, Sunnyvale, CA, USA).

Abnormal behavior observation

Mice were subjected to a battery of vestibular evaluations, including observation of their circling behavior and head-tilting, and a tail-hanging test (Kim et al., 2012). One hundred and one mice consisting of 78 homozygotes, 14 heterozygotes, and nine wild-type mice were checked for abnormal behavior display of circling and head-tilting. For the tail-hanging test, visual cues were blocked by putting terramycin ophthalmic ointment (Terramycin eye ointment®, Pfizer Pharm. Korea, Seoul, Korea) on both eyes before the test and proprioception was blocked by

hanging a tail. A high speed camera (FMVU-0.3MTC-CS; Point Grey Research Inc., Richmond, BC, Canada) was used to record the twist motion, and an algorithm was designed for the tail-hanging test to differentiate the twist motion. Open CV v1.0 (Microsoft®, Redmond, WA, USA) was used as programming tools. The basis of the tracking algorithm is the image subtraction of a reference video frame from subsequent video frames containing a moving object.

RESULTS

Auditory brainstem response thresholds: all-or-none

We measured auditory brainstem response thresholds for each ear of experimental *Slc26a4*$^{+/+}$, *Slc26a4*$^{\Delta/+}$, Tg(+);*Slc26a4*$^{\Delta/\Delta}$ and *Slc26a4*$^{\Delta/\Delta}$ at 3 months of age. Average auditory brainstem response thresholds of right ears were significantly elevated (*P<0.05*) in *Slc26a4*$^{\Delta/\Delta}$ mice (n=8) at 120 ± 0 dB SPL (sound pressure level), compared with Tg(+);*Slc26a4*$^{\Delta/\Delta}$ (n=13) at 32.3 ± 7.3 dB SPL, *Slc26a4*$^{\Delta/+}$ (n=10) at 28.0 ± 7.9 dB SPL, and wild type *Slc26a4*$^{+/+}$ mice (n=9) at 26.7 ± 7.1 dB SPL (Fig. 1). All *Slc26a4*$^{\Delta/\Delta}$ mice had profound deafness, whereas there were no differences of hearing thresholds between Tg(+);*Slc26a4*$^{\Delta/\Delta}$, *Slc26a4*$^{\Delta/+}$, and *Slc26a4*$^{+/+}$ mice. As proven, the all-or-none pattern of hearing status in pendrin-deficient mice was clearly pronounced.

Vestibular dysfunction: dose-dependent VOR responses

The mean gains of earth vertical–horizontal rotation at 0.1 Hz, with a peak velocity of 100°/s, were as follows: 0.87 ± 0.03 in *Slc26a4*$^{+/+}$, 0.75 ± 0.02 in *Slc26a4*$^{\Delta/+}$, 0.57 ± 0.03 in Tg(+);*Slc26a4*$^{\Delta/\Delta}$, 0.03 ± 0.02 in *Slc26a4*$^{\Delta/\Delta}$, and 0.50 ± 0.02 in mice with right unilateral labyrinthectomy (Fig. 2A). There was a significant difference of mean gains between Tg(+);*Slc26a4*$^{\Delta/\Delta}$ and *Slc26a4*$^{\Delta/\Delta}$ mice (*P*<0.05). The mean gain of the Tg(+);*Slc26a4*$^{\Delta/\Delta}$ mice was intermediate between *Slc26a4*$^{\Delta/+}$ and *Slc26a4*$^{\Delta/\Delta}$ mice. The mean gain of the *Slc26a4*$^{\Delta/+}$ mice was intermediate between *Slc26a4*$^{+/+}$

and Tg(+);*Slc26a4*$^{\Delta/\Delta}$ mice (P<0.05). These pendrin dose-dependent patterns of VOR responses were also seen at 0.2 Hz (Fig. 2B) and at 0.5 Hz (Fig. 2C), with peak velocity of 100°/s. For *Slc26a4*$^{\Delta/\Delta}$ mice, near zero responses were recorded at each frequency of sinusoidal harmonic acceleration test. Both Tg(+);*Slc26a4*$^{\Delta/\Delta}$ and *Slc26a4*$^{\Delta/+}$ mice exhibited higher gains with the increase of stimulus frequency. Values for Tg(+);*Slc26a4*$^{\Delta/\Delta}$ mice were 0.57 ± 0.03 at 0.1 Hz, 0.63 ± 0.03 at 0.2 Hz, and 0.68 ± 0.03 at 0.5 Hz, and the values for *Slc26a4*$^{\Delta/+}$ mice were 0.75 ± 0.02 at 0.1 Hz, 0.76 ± 0.02 at 0.2 Hz, and 0.81 ± 0.02 at 0.5 Hz. The mean gains of the wild types were 0.87 ± 0.03 at 0.1 Hz, 0.92 ± 0.02 at 0.2 Hz, and 0.90 ± 0.03 at 0.5 Hz; and that for mice with unilateral labyrinthectomy were 0.50 ± 0.02 at 0.1 Hz, 0.50 ± 0.02 at 0.2 Hz, and 0.52 ± 0.03 at 0.5 Hz.

Anatomical abnormality of LSC

Figure 3 shows the results of anti-pendrin immunostaining of the LSC ampulla of mice with pendrin deficiency. We were able to detect strong pendrin immunoreactivity in non-sensory epithelial cells surrounding the sensory hair-cell patches in ampullae of *Slc26a4*$^{+/+}$ ears. However, the level of staining in *Slc26a4*$^{\Delta/+}$ was lower than that in *Slc26a4*$^{+/+}$ controls and bigger than that in Tg(+);*Slc26a4*$^{\Delta/\Delta}$ mice. There was no detectable immunoreactivity in the *Slc26a4*$^{\Delta/\Delta}$ ampullae. These results demonstrate an uneven, but pendrin dose-dependent expression of the pendrin protein in mice with various *SLC26A4* genotypes.

Grossly, the long LSC ampulla diameter in the *Slc26a4*$^{\Delta/\Delta}$ increased by 20%

compared with *Slc26a4*$^{+/+}$ mice. There was no macroscopic difference of LSC ampulla between *Slc26a4*$^{\Delta/+}$ and *Slc26a4*$^{+/+}$. All of the Tg(+);*Slc26a4*$^{\Delta/\Delta}$ mice had normal gross semicircular canal anatomy. The histology of the LSC showed that a substantial portion of vestibular hair cells from *Slc26a4*$^{\Delta/\Delta}$ were replaced by vacuoles, while there was no apparent difference in hair cell architectures and hair cell populations between *Slc26a4*$^{+/+}$, *Slc26a4*$^{\Delta/+}$, and Tg(+);*Slc26a4*$^{\Delta/\Delta}$ mice (Fig. 4). In immunohistochemistry, the expression of calretinin was absent in the *Slc26a4*$^{\Delta/\Delta}$ ampulla. On the other hand, the expression of calretinin, which mainly occurs in type I vestibular hair cells, was clearly observed in *Slc26a4*$^{+/+}$, *Slc26a4*$^{\Delta/+}$, and Tg(+);*Slc26a4*$^{\Delta/\Delta}$ ampullae (Fig. 5). No apparent difference of calretinin expression was observed between *Slc26a4*$^{+/+}$, *Slc26a4*$^{\Delta/+}$, and Tg(+);*Slc26a4*$^{\Delta/\Delta}$.

Endolymphatic potentials from the LSC

Electrophysiological difference between *Slc26a4*$^{+/+}$ (n=4), *Slc26a4*$^{\Delta/+}$ (n=4) and *Slc26a4*$^{\Delta/\Delta}$ (n=4) was investigated by measuring the potentials from LSC in 12 mice. There was no significant difference of mean value of the endolymphatic potentials between three groups; -6.15 ± 1.03 mV in *Slc26a4*$^{+/+}$, -6.60 ± 1.05 mV in *Slc26a4*$^{\Delta/+}$, and -5.30 ± 1.18 mV in *Slc26a4*$^{\Delta/\Delta}$ ($P>0.05$).

Behavioral phenotype

Head-tilting was observed in all 78 (100%) *Slc26a4*$^{\Delta/\Delta}$ mice and circling behavior was observed in 14 (17.9%). There was neither tilting nor circling mice in

Tg(+);*Slc26a4*$^{\Delta/\Delta}$, *Slc26a4*$^{\Delta/+}$, and *Slc26a4*$^{+/+}$. In the tail-hanging test, the difference of mean minimum sway angle between *Slc26a4*$^{\Delta/+}$ with twisting motion and *Slc26a4*$^{\Delta/\Delta}$ with anterior bending was significant (Fig. 6). No difference of mean minimum sway angle was observed between *Slc26a4*$^{+/+}$ and *Slc26a4*$^{\Delta/+}$, as well as between *Slc26a4*$^{+/+}$ and *Slc26a4*$^{\Delta/\Delta}$. All minimal sway angles of mice with unilateral labyrinthectomy were <100° because of their spinning movement during the tail-hanging test. The mean minimal sway angle of them was significantly higher than those of *Slc26a4*$^{+/+}$, *Slc26a4*$^{\Delta/+}$, and *Slc26a4*$^{\Delta/\Delta}$.

DISCUSSION

The horizontal VOR response for the LSC is essential to stabilize eye position in space during head movement. The VOR results of *Slc26a4*$^{+/+}$ control mice were qualitatively similar to other studies in mice using both search coil (Harrod and Baker, 2003) and video-nystagmography (Migliaccio et al., 2011). In the *Slc26a4*$^{\Delta/\Delta}$ mice, even those with relatively enlarged LSC morphology, there were only near zero responses to any rotational stimuli tested for VOR. Although Tg(+)*;Slc26a4*$^{\Delta/\Delta}$ and *Slc26a4*$^{\Delta/+}$ mice exhibited no LSC behavioral or anatomical abnormalities, VOR responses demonstrated an intermediate phenotype. The VOR pattern of mice with various *Slc26a4* genotypes corresponds to the amount of expression of pendrin in the LSC ampulla, implying dose-dependent phenomenon of mean VOR gains in order of pendrin sufficiency; *Slc26a4*$^{+/+}$, *Slc26a4*$^{\Delta/+}$, Tg(+);*Slc26a4*$^{\Delta/\Delta}$ and *Slc26a4*$^{\Delta/\Delta}$. Sinusoidal harmonic acceleration stimulation showed significant differences of VOR gains between *Slc26a4*$^{+/+}$, *Slc26a4*$^{\Delta/+}$, and Tg(+);*Slc26a4*$^{\Delta/\Delta}$ mice, suggesting that there is some vestibular dysfunction even in *Slc26a4*$^{\Delta/+}$ and Tg(+);*Slc26a4*$^{\Delta/\Delta}$ mice. On the other hand, ABR thresholds of *Slc26a4*$^{\Delta/+}$ and Tg(+);*Slc26a4*$^{\Delta/\Delta}$ were within normal limit, indicating that the presence of any amount of pendrin allows the achievement of normal hearing. In addition, all homozygotes had total deafness, showing all-or-none character of pendrin for auditory function in the mouse model; this is consistent with previously reported studies (Choi et al., 2011; Everett et al., 2001). Although there was an attempt to

exclude influence of anesthesia while evaluating horizontal nystagmus, an overestimation of degree and prevalence of VOR hypo-responsiveness may have existed. We concluded that vestibular function through VOR of LSC is manifested with a pendrin dose-dependent pattern, while auditory function shows all-or-none phenotype in pendrin-deficient mice.

Previous study proposed that a bi-transgenic mouse line, in which the expression of *Slc26a4* was inducible by doxycycline (Tg(+);*Slc26a4*$^{\Delta/\Delta}$), was made to activate and deactivate *Slc26a4* expression reversibly in order to assess the temporal requirements for pendrin in the inner ear (Choi et al., 2011). The restoration of pendrin prevented hearing loss and balance functions through the recovery of a normal endocochlear potential, normal pH gradients between endolymph and perilymph in the cochlea, and normal otoconia formation in the vestibular labyrinth (Choi et al., 2011; Ito et al., 2014; Li et al., 2013). In such study, Tg(+);*Slc26a4*$^{\Delta/\Delta}$ mice showed normal hearing levels but decreased VOR responses compare with both normal and heterozygotes controls. This finding conflicts the expected outcome as the previous report of normal hearing and balance function in Tg(+);*Slc26a4*$^{\Delta/\Delta}$ mice (Li et al., 2013). *Slc26a4* heterozygous mice also had normal hearing but VOR responses were lower than normal controls, but higher than Tg(+);*Slc26a4*$^{\Delta/\Delta}$, contradicting previous reports (Everett et al., 2001; Li et al., 2013) and pattern of autosomal recessive inheritance of *SLC26A4* gene. As observed, some vestibular hypofunction occurred in the presence of pendrin expression in the LSC. In addition, heterozygotes had intermediate VOR responses

compared with homozygotes and normal controls; all types were knockout-mouse models with an autosomal recessive disorder (Makishima et al., 2011). Therefore, we can assume that the amount of pendrin in the vestibule is not enough to maintain the physiological status of the inner ears of *Slc26a4*$^{\Delta/+}$ and Tg(+);*Slc26a4*$^{\Delta/\Delta}$ mice. Discrepancies between our findings and other studies seem to have derived from the difference in the methods of balance test. We used rotational test, in which the stimulation of horizontal nystagmus could be recorded to evaluate the direct VOR pathways. The use of rotarod test for demonstrating the ability to balance on an accelerating rotating rod (Everett et al., 2001; Li et al., 2013) might result in interpretation errors; this is because there may be influences from various factors such as emotion, locomotion, or cognition rather than actual vestibular function. Even if Tg(+);*Slc26a4*$^{\Delta/\Delta}$ and *Slc26a4*$^{\Delta/+}$ mice acquired normal balancing on a rotating rod, dose-dependent VOR patterns to rotation stimulation in our mice strain emphasized delicate vestibular problems of pendrin deficiency.

Vestibular mutant homozygous mice with abnormal VOR responses also had profound deficits of posture and locomotion, not only in pendrin-deficient model (Everett et al., 2001; Li et al., 2013), but also in other protein-deficient models (Makishima et al., 2011; Vidal et al., 2004). All *Slc26a4*$^{\Delta/\Delta}$ mice with abnormal VOR and complete hearing loss showed head-tilting behavior, although not all (17.9%) of them had circling episode in the present study. The extent to which peripheral vestibular mechanisms contributes to the circling movement remains unclear. Some authors proclaim that the direction of circling in homozygotes

corresponded to the extent of hypomorphism of vestibule (Makishima et al., 2011). Little VOR response and no VOR asymmetry of our *Slc26a4*$^{\Delta/\Delta}$ raised the possibility that asymmetrical central compensation of bilateral vestibulopathy in *Slc26a4* homozygous mice might have triggered the unidirectional circling behavior towards the more uncompensated vestibule. Further functional and histological studies on the inner ear and central vestibular systems are needed to clarify this question. Subtle distinctions of minimum sway angle in the tail-hanging test support that *Slc26a4* homozygote and heterozygotes had different kinds of vestibular dysfunction, particularly when the influences of somatosensory inputs were excluded. In a strict sense, these are involved in the vestibulo-spinal reflex, not the VOR pathway. Mice with unilateral labyrinthectomy had ipsilateral deafness and contralateral normal hearing. Mean VOR gains of these mice were approximately 0.5 at all frequencies in sinusoidal harmonic acceleration test and their minimum sway angles were all <100° due to spinning behavior in the tail-hanging test. The mice were considered as a counterpart with a unilateral vestibulopathy because *Slc26a4*$^{\Delta/\Delta}$ mice were expected to have bilateral vestibular hypofunction.

It is known that transitional cells surrounding the vestibular neuroepithelia in semicircular canals and otolithic organs, spindle cells of the stria vascularis in cochlea, and mitochondria-rich cells in the endolymphatic sac manifest pendrin in wild type mice. Therefore, lack of pendrin-immunoreactivity can be observed in all of these locations in the *Slc26a4*$^{\Delta/\Delta}$ homozygotes (Choi et al., 2011; Dou et al., 2004; Li et al., 2013; Royaux et al., 2001). Many authors believe that pendrin in

these cells contributes to pH and ionic homeostasis of endolymph, which is the potassium-rich fluid filling the vestibule, cochlea, and endolymphatic duct. Endolymph flows through the mechano-sensory stereocilia bundles of the vestibular and cochlear hair cells, and the maintenance of its ionic composition and pH is mandatory to send signals of hearing and balance (Li et al., 2013; Richardson et al., 2011). In this study, pendrin was expressed in non-sensory epithelial cells surrounding the sensory hair-cell patches in the LSC ampullae of wild type, *Slc26a4*$^{\Delta/+}$ and Tg(+); *Slc26a4*$^{\Delta/\Delta}$ mice.

Ultrastructural studies exhibited additional insights about the potential role of pendrin in the LSC. For example, the deficiency of pendrin may account for the deformation of hair cell architectures and the replacement with vacuoles seen in *Slc26a4*$^{\Delta/\Delta}$. Vacuoles are thought to be formed by damages in the vestibular sensory epithelium secondary to biochemical alterations of the endolymph. The absence of pendrin also appeared to evoke the lack of calretinin from the type I vestibular hair cells in the LSC of *Slc26a4*$^{\Delta/\Delta}$. These histologic changes in homozygotes did not happen in heterozygous and transgenic mice. A mismatch between the LSC anatomy and the VOR function was similar to heterozygotes of other knockout mice (Makishima et al., 2011), but different from Tg(+);*Slc26a4*$^{\Delta/\Delta}$ of the same animal model (Li et al., 2013). There was no difference of vestibular hair cell numbers in the LSC ampuala between wild type, *Slc26a4*$^{\Delta/+}$ and Tg(+); *Slc26a4*$^{\Delta/\Delta}$ mice, although the data were not shown in this study. One possible explanation for the mechanism of dose-dependent VOR responses without anatomical abnormality is

that *Slc26a4*$^{\Delta/+}$ and Tg(+);*Slc26a4*$^{\Delta/\Delta}$ failed to achieve normal endolymphatic potential or pH in the ampulla of the semicircular canals, which caused improper functional development. Reduced endocochlear potential and decreased endolymphatic pH in transgenic mice, compared with *Slc26a4*$^{\Delta/+}$ (Choi et al., 2011), implies the above explanation partially. However, precise measurement of the endolymphatic potential and pH in the LSC ampulla was not easy in a technical aspect. We expected that the amplitude of the endolymphatic potentials from LSC of homozygotes is different from that of normal controls, but there was no statistical difference of mean amplitude of the potentials between between *Slc26a4*$^{+/+}$, *Slc26a4*$^{\Delta/+}$ and *Slc26a4*$^{\Delta/\Delta}$. This can infer decreased VOR responses in *Slc26a4*$^{\Delta/\Delta}$ and *Slc26a4*$^{\Delta/+}$ derive from not endolymphatic space of semicircular canal but other sites, such as vestibular nerve endings or synapses.

All *Slc26a4*$^{\Delta/\Delta}$ mouse models show prominent microscopic anomalies of otolithic organs in the inner ear (Dror et al., 2010; Everett et al., 2001; Lu et al., 2011). A closer look at the utricle and saccule of these mouse models reveals giant otoliths abnormally associated with the vestibular sensory epithelium (Dror et al., 2010; Everett et al., 2001). The formation of the giant otoconia destroys the equilibrium between otoconia and the underlying hair cells. In normal conditions, the otoconia sustains an equally distributed mass to elicit the hair cells; in the presence of *Slc26a4* mutations, a sporadic distribution of the giant minerals leads to a differential mass over the sensory cells. Whereas some hair cells are overloaded with the weight of the giant stones, others lack any viable load of otoconia minerals.

Therefore, both cell populations are neutralized from being active in vestibular sensation and lead to severely disturbed vestibular perception (Dror et al, 2011). Because there was emphasis in the LSC and the horizontal VOR angular acceleration, evaluations of saccule and utricle for linear acceleration and gravity were entirely omitted in this study. Nevertheless, it is important to keep in mind that the balance system consists of three semicircular canals and two otolithic organs in each ear and there are extensive interactions among them and the central nervous system. In this study, mice at 2–3 months of age were used in order to avoid age-related changes known to affect the C57BL6 mice background strain. In C57BL6 mice, VOR gains and histological changes in the vestibular organ occur after 6 months of age (Shiga et al., 2005). Further vestibular function analysis and histological studies in mice at different ages may be elucidated in this mouse model.

CONCLUSIONS

Pendrin-deficient mice showed pendrin dose-dependent VOR responses of LSC, as well as all-or-none phenotype for audiologic function. Mutations of *Slc26a4* gene induce anatomical and functional deficits of vestibular hair cells in the LSC ampulla. The results in this study, together with those of previous inner ear studies on *Slc26a4*$^{\Delta/\Delta}$ mice, indicate that pendrin is essential for the normal function of the auditory and vestibular system and also for the LSC morphogenesis.

REFERENCES

Adams KM, Abraham V, Spielman D, Kolls JK, Rubenstein RC, Conner GE et al. IL-17A induces Pendrin expression and chloride-bicarbonate exchange in human bronchial epithelial cells. PLoS One 2014;9(8);e103263.

Alesutan I, Daryadel A, Mohebbi N, Pelzl L, Leibrock C, Voelkl J, et al. Impact of bicarbonate, ammonium chloride, and acetazolamide on hepatic and renal *SLC26A4* expression. Cell Physiol Biochem 2011;28(3):553-8.

Baizer JS and Broussard DM. Expression of calcium-binding proteins and nNOS in the human vestibular and precerebellar brainstem. J Comp Neurol 2010;518(6):872-95.

Bidart JM, Lacroix L, Evain-Brion D, Caillou B, Lazar V, Frydman R, et al. Expression of Na+/I- symporter and Pendred syndrome genes in trophoblast cells. J Clin Endocrinol Metab 2000;85(11):4367-72.

Choi, BY, Kim HM, Ito T, Lee KY, Li X, Monahan K et al. Mouse model of enlarged vestibular aqueducts defines temporal requirement of *Slc26a4* expression for hearing acquisition. J Clin Invest 2011;121(11):4516-25.

Dossena S, Rodighiero S, Vezzoli V, Bazzini C, Sironi C, Meyer G, et al. Fast fluorometric method for measuring pendrin (*SLC26A4*) Cl^-/I^- transport activity. Cell Physiol Biochem 2006;18(1-3):67-74.

Dou H, Xu J, Wang Z, Smith AN, Soleimani M, Karet FE, et al. Co-expression of pendrin, vacuolar H^+-ATPase alpha4-subunit and carbonic anhydrase II in epithelial

cells of the murine endolymphatic sac. J Histochem Cytochem 2004;52(10):1377-84.

Dror AA, Brownstein Z, Avraham KB. Integration of human and mouse genetics reveals pendrin function in hearing and deafness. Cell Physiol Biochem 2011;28(3):535-44.

Dror AA, Politi Y, Shahin H, Lenz DR, Dossena S, Nofziger C, et al. Calcium oxalate stone formation in the inner ear as a result of an *Slc26a4* mutation. J Biol Chem 2010;285(28):21724-35.

Everett LA, Belyantseva IA, Noben-Trauth K, Cantos R, Chen A, Thakkar SI, et al. Targeted disruption of mouse Pds provides insight about the inner-ear defects encountered in Pendred syndrome. Hum Mol Genet 2001;10(2):153-61.

Griffith A J, Arts A, Downs C, Innis JW, Shepard NT, Sheldon S, et al. Familial large vestibular aqueduct syndrome. Laryngoscope 1996;106(8):960-65.

Harrod CG and Baker JF. The vestibulo ocular reflex (VOR) in otoconia deficient head tilt (het) mutant mice versus wild type C57BL/6 mice. Brain Res 2003;972(1-2):75-83.

Ito T, Li X, Kurima K, Choi BY, Wangemann P, Griffith AJ. *Slc26a4*-insufficiency causes fluctuating hearing loss and stria vascularis dysfunction. Neurobiol Dis 2014;66:53-65.

Kim HM and Wangemann P. Epithelial cell stretching and luminal acidification lead to a retarded development of stria vascularis and deafness in mice lacking pendrin. PLoS One 2011;6(3):e17949.

Kim MJ, Kim NB, Lee EJ, Han GC. “Tail-hanging test” behavioral parameter of vestibular deficit and compensation in labyrinthectomized mouse model. Int Adv Otol 2012;8(3):453-62.

King KA, Choi BY, Zalewski C, Madeo AC, Manichaikul A, Pryor SP et al. *SLC26A4* genotype, but not cochlear radiologic structure, is correlated with hearing loss in ears with an enlarged vestibular aqueduct. Laryngoscope 2010;120(2):384-89.

Lee HH, Kim MJ, Jo YK, Kim JY, Han GC. Vestibular effects of lidocaine intratympanic injection in rats. Hum Exp Toxicol 2014;33(11):1121-33.

Li X, Sanneman JD, Harbidge DG, Zhou F, Ito T, Nelson R et al. *SLC26A4* targeted to the endolymphatic sac rescues hearing and balance in *Slc26a4* mutant mice. PLoS Genet 2013;9(7):e1003641.

Lu YC, Wu CC, Shen WS, Yang TH, Yeh TH, Chen PJ et al. Establishment of a knock-in mouse model with the *SLC26A4* c.919-2A>G mutation and characterization of its pathology. PLoS One 2011;6(7):e22150.

Makishima T, Hochman L, Armstrong P, Rosenberger E, Ridley R, Woo M et al. Inner ear dysfunction in caspase-3 deficient mice. BMC Neurosci 2011;12:102.

Migliaccio AA, Meierhofer R, Della Santina CC. Characterization of the 3D angular vestibulo-ocular reflex in C57BL6 mice. Exp Brain Res 2011;210(3-4):489-501.

Miyagawa M, Nishio SY, Usami S. Mutation spectrum and genotype-phenotype correlation of hearing loss patients caused by *SLC26A4* mutations in the Japanese: a large cohort study. J Hum Genet 2014;59(5):262-8.

Nakao I, Kanaji S, Ohta S, Matsushita H, Arima K, Yuyama N et al. Identification of pendrin as a common mediator for mucus production in bronchial asthma and chronic obstructive pulmonary disease. J Immunol 2008;180(9):6262-9.

Noben-Trauth K, Latoche JR, Neely HR, Bennett B. Phenotype and genetics of progressive sensorineural hearing loss (Snhl1) in the LXS set of recombinant inbred strains of mice. PLoS One 2010;5(7):e11459.

Nofziger C, Vezzoli V, Dossena S, Schonherr T, Studnicka J, Nofziger J et al. STAT6 links IL-4/IL-13 stimulation with pendrin expression in asthma and chronic obstructive pulmonary disease. Clin Pharmacol Ther 2011;90(3):399-405.

Pedemonte N, Caci E, Sondo E, Caputo A, Rhoden K, Pfeffer U et al. Thiocyanate transport in resting and IL-4-stimulated human bronchial epithelial cells: role of pendrin and anion channels. J Immunol 2007;178(8):5144-53.

Pelzl L, Pakladok T, Pathare G, Fakhri H, Michael D, Wagner CA et al. DOCA sensitive pendrin expression in kidney, heart, lung and thyroid tissues. Cell Physiol Biochem 2012;30(6):1491-501.

Pryor SP, Madeo AC, Reynolds JC, Sarlis NJ, Arnos KS, Nance WE et al. *SLC26A4/PDS* genotype-phenotype correlation in hearing loss with enlargement of the vestibular aqueduct (EVA): evidence that Pendred syndrome and non-syndromic EVA are distinct clinical and genetic entities. J Med Genet 2005;42(2):159-165.

Richardson GP, de Monvel JB, Petit C. How the genetics of deafness illuminates auditory physiology. Annu Rev Physiol 2011;73:311-34.

Royaux IE, Wall SM, Karniski LP, Everett LA, Suzuki K, Knepper MA et al. Pendrin, encoded by the Pendred syndrome gene, resides in the apical region of renal intercalated cells and mediates bicarbonate secretion. Proc Natl Acad Sci USA 2001;98(7):4221-6.

Scott DA, Wang R, Kreman TM, Sheffield VC, Karniski LP. The Pendred syndrome gene encodes a chloride-iodide transport protein. Nat Genet 1999;21(4):440-3.

Shiga A, Nakagawa T, Nakayama M, Endo T, Iguchi F, Kim TS et al Aging effects on vestibulo-ocular responses in C57BL/6 mice: comparison with alteration in auditory function. Audiol Neurootol 2005;10(2):97-104.

Soleimani M, Greeley T, Petrovic S, Wang Z, Amlal H, Kopp P et alPendrin: an apical Cl-/OH-/HCO3- exchanger in the kidney cortex. Am J Physiol Renal Physiol 2001;280(2):F356-364.

Stinckens C, Huygen PL, Joosten FB, Van Camp G, Otten B, Cremers CW. Fluctuant, progressive hearing loss associated with Meniere like vertigo in three patients with the Pendred syndrome. Int J Pediatr Otorhinolaryngol 2001;61(3): 207-15.

Sugiura M, Sato E, Nakashima T, Sugiura J, Furuhashi A, Yoshino T et al. Long-term follow-up in patients with Pendred syndrome: vestibular, auditory and other phenotypes. Eur Arch Otorhinolaryngol 2005;262(9):737-43.

Vidal PP, Degallaix L, Josset P, Gasc JP, Cullen KE. Postural and locomotor control in normal and vestibularly deficient mice. J Physiol 2004;559(2):625-38.

Wangemann P, Nakaya K, Wu T, Maganti RJ, Itza EM, Sanneman JD et al. Loss of cochlear HCO3- secretion causes deafness via endolymphatic acidification and inhibition of Ca2+ reabsorption in a Pendred syndrome mouse model. Am J Physiol Renal Physiol 2007;292(5):F1345-53.

Zalewski CK, Chien WW, King KA, Muskett JA, Baron RE, Butman JA et al. Vestibular Dysfunction in Patients with Enlarged Vestibular Aqueduct. Otolaryngol Head Neck Surg 2015;153(2):257-62.

Fig.1. Mean auditory brainstem response thresholds of right ears in response to a click stimulus. Mean ± SD thresholds of right ears are shown. Numerals in parenthesis next to data points indicate the number of tested mice for each group. Mean thresholds are also listed in numerals. Note that all *Slc26a4* homozygous knockout mice showed total deafness, whereas the others had normal hearing, indicating the all-or-none phenotype of auditory function. Tg(+): transgenic mice with doxycycline-inducible expression of *Slc26a4*.

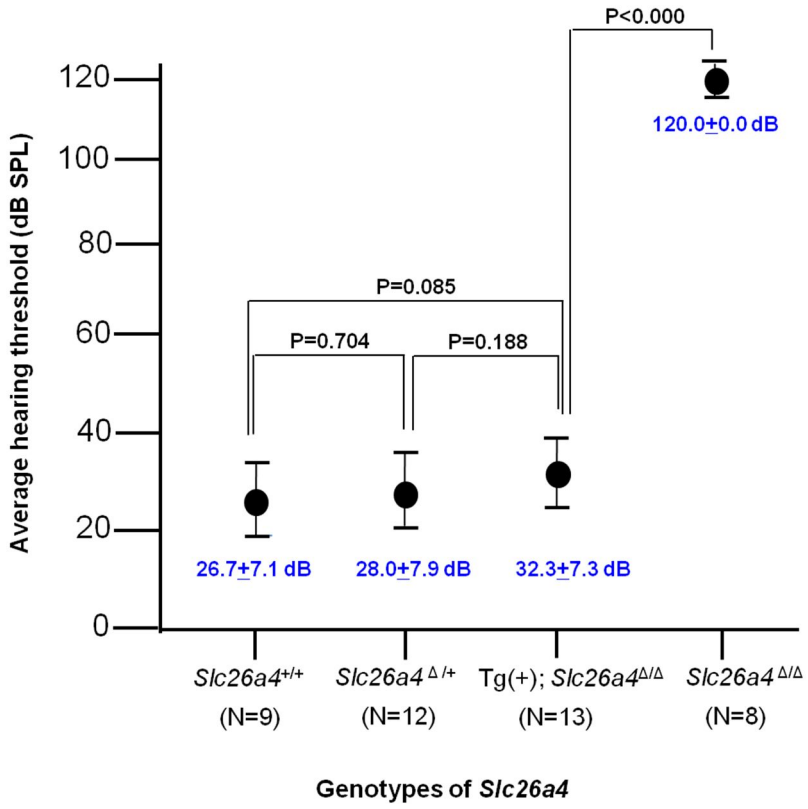

Fig.2. The VOR gains at 100°/s-peak velocity: (A) 0.1, (B) 0.2, and (C) 0.5 Hz oscillation stimulations were achieved from *Slc26a4* variation models and right side unilateral labyrinthectomy model. Each subject group showed significantly different gain. The mean gain of Tg(+);*Slc26a4*$^{\Delta/\Delta}$ was intermediate to gains of *Slc26a4*$^{\Delta/+}$ and *Slc26a4*$^{\Delta/\Delta}$. The same phenomenon was found at all test frequencies. Tg(+): transgenic mice with doxycycline-inducible expression of *Slc26a4*; ULx: mice with unilateral labyrinthectomy.

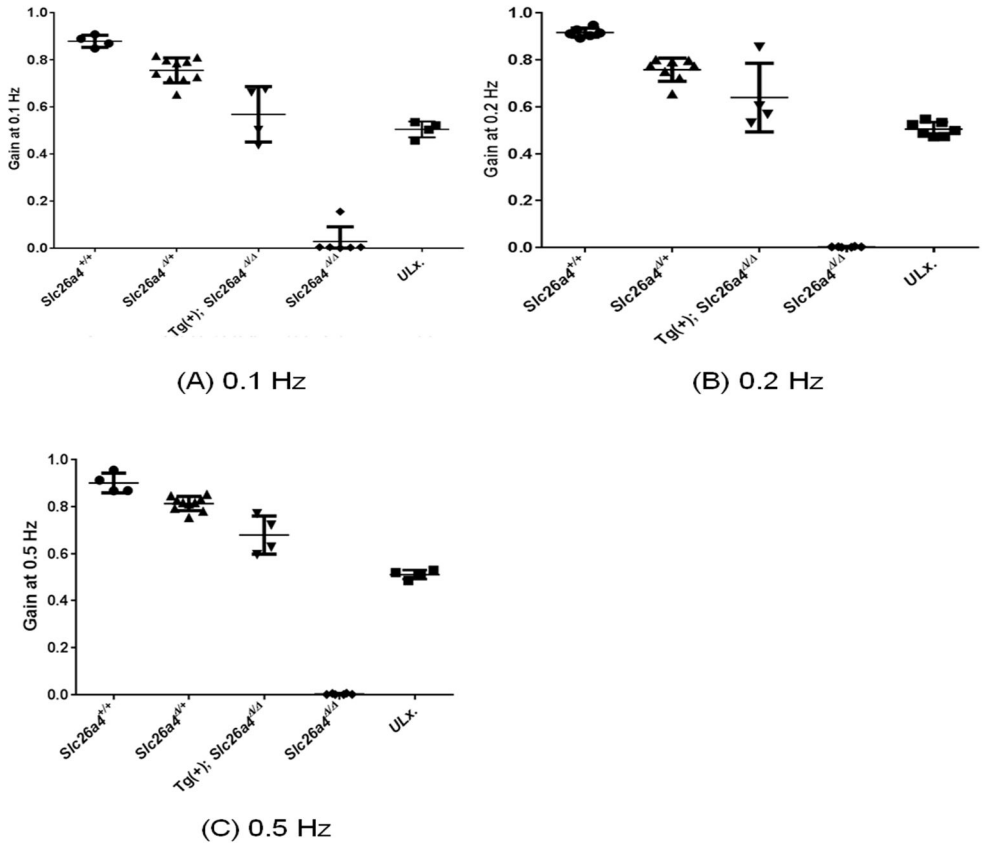

Fig.3. Differences in the amount of pendrin expression among the ampulla of the LSC of mice with various *Slc26a4* genotypes: (A) *Slc26a4*$^{+/+}$, (B) *Slc26a4*$^{\Delta/+}$, (C) Tg(+);*Slc26a4*$^{\Delta/\Delta}$, and (D) *Slc26a4*$^{\Delta/\Delta}$ with schematic diagram of the ampulla (E). White scale bars: 50 μm. Pendrin is expressed in nonsensory epithelial cells surrounding the sensory hair-cell patches in (A), (B), and (C); not in (D). EC: eminentia cruciata, HC: vestibular hair cells, TC: transitional cells, C: cupula. A red arrow in (E) indicates the point of whole-mounted view for (A), (B), (C), and (D).

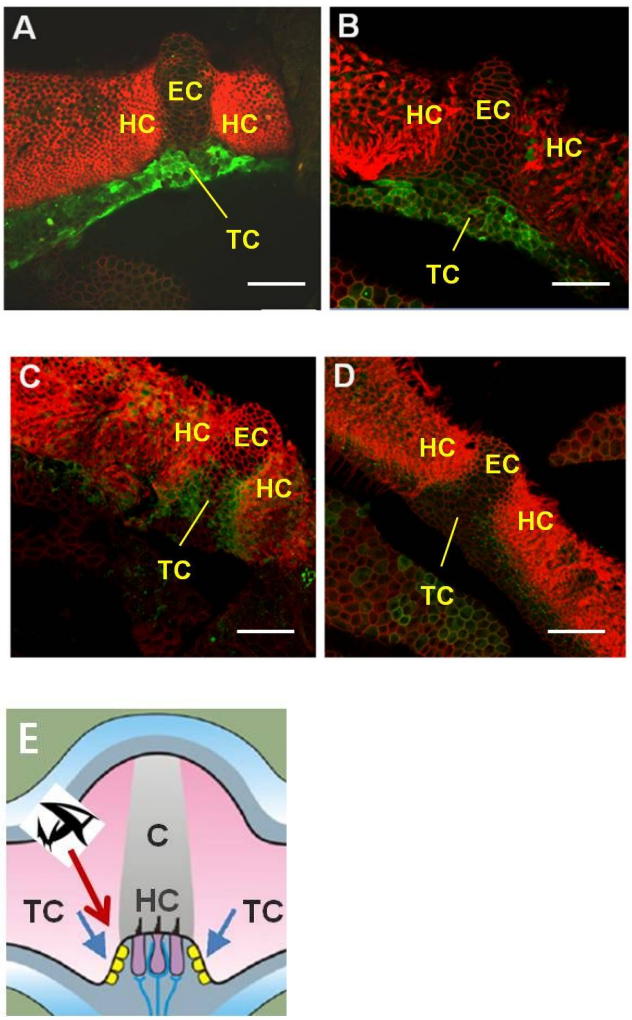

Fig.4. Comparison of microanatomy among mice with various *Slc26a4* genotypes: (A and B) *Slc26a4*$^{+/+}$, (C and D) *Slc26a4*$^{\Delta/+}$, (E and F) Tg(+);*Slc26a4*$^{\Delta/\Delta}$, and (G and H) *Slc26a4*$^{\Delta/\Delta}$. Black scale bars: 50 μm. Note that a substantial portion of vestibular hair cells (surrounded by blue line) from *Slc26a4*$^{\Delta/\Delta}$ are replaced by vacuoles (black arrows), while there is no apparent difference in hair cell architectures and hair cell populations between *Slc26a4*$^{+/+}$, *Slc26a4*$^{\Delta/+}$, and Tg(+);*Slc26a4*$^{\Delta/\Delta}$ mice.

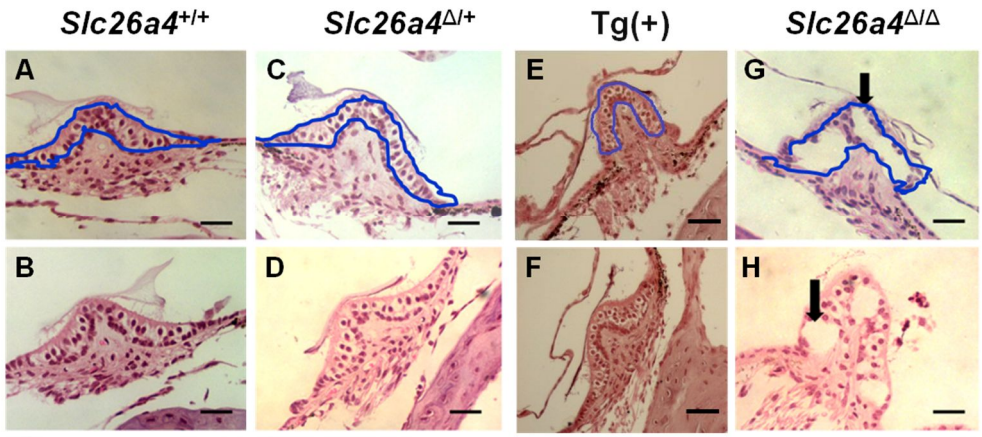

Fig.5. Differences in the expression of calretinin among mice with various *Slc26a4* genotypes: (A) *Slc26a4*$^{+/+}$, (B) *Slc26a4*$^{\Delta/+}$, (C) Tg(+);*Slc26a4*$^{\Delta/\Delta}$, and (D) *Slc26a4*$^{\Delta/\Delta}$. White scale bars: 50 μm. Note that the absence of calretinin expression from vestibular hair cells of *Slc26a4*$^{\Delta/\Delta}$ while expression of calretinin (white arrows), which is mainly expressed from the type I vestibular hair cells, is clearly observed from hair cells of *Slc26a4*$^{+/+}$, *Slc26a4*$^{\Delta/+}$, and Tg(+);*Slc26a4*$^{\Delta/\Delta}$. No apparent difference between *Slc26a4*$^{+/+}$, *Slc26a4*$^{\Delta/+}$, and Tg(+);*Slc26a4*$^{\Delta/\Delta}$ can be observed.

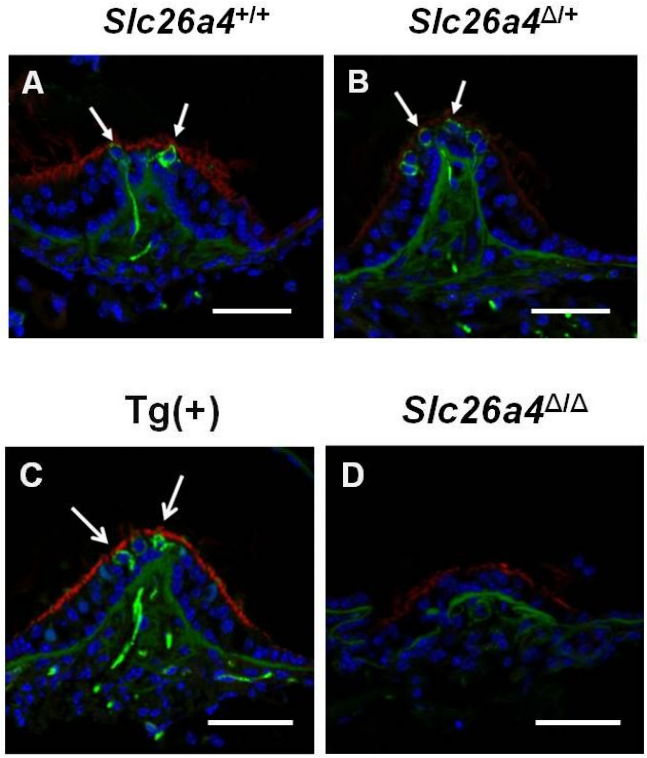

Fig.6. Differences of minimal body sway angles of mice with various *Slc26a4* genotypes in the tail-hanging test. There was a significant difference of minimal sway angle between *Slc26a4* homozygotes and heterozygotes (*, *P<0.05*). Minimal sway angles of mice with unilateral labyrinthectomy (ULx) were <100°/s (***, P<0.001).

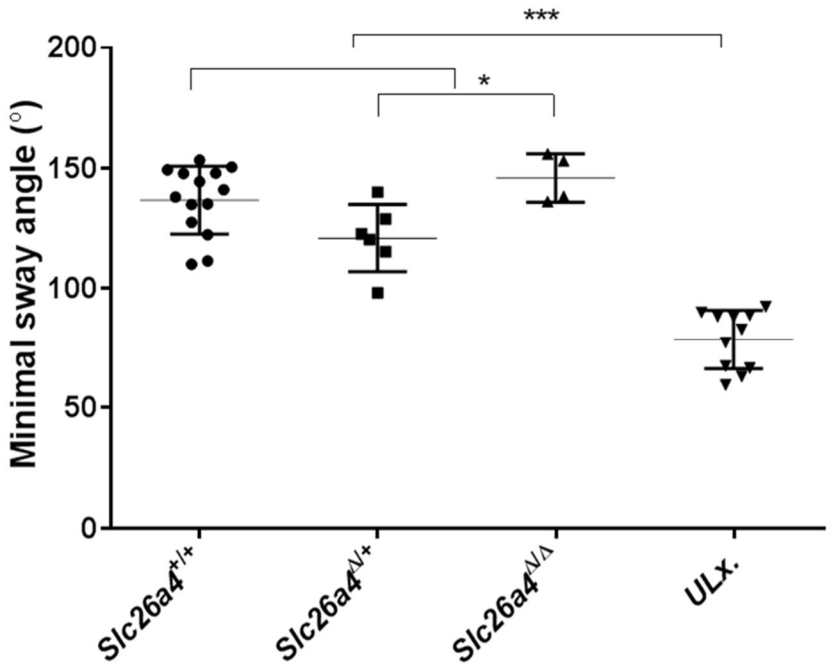

국문초록

SLC26A4 유전자에 의해 발현되는 펜드린은 내이의 상피세포에서 발견되는 음이온 교환 단백질이다. 펜드린 결핍은 임상적으로 전정수도관 확장증과 관련된 난청을 유발하고, 동시에 어지럼증과 자세 불균형을 일으킨다. 이에 대해 본 연구는 펜드린 결핍 마우스 모델에서 외반고리관의 해부학적 이상과 전정-안구 반사의 정량적인 반응에 대해 조사하였다. 마우스 모델은 1) 동형접합성 유전자결핍 마우스, 2) 독시싸이클린으로 *Slc26a4* 유전자가 유도 가능한 형질변환 마우스, 3) 이형접합성 유전자결핍 마우스의 세 가지 서로 다른 뚜렷한 유전적 조건과 정상 대조군 마우스로 구성되었다. 청력과 균형 감각은 청성 뇌간 반응 검사, 정현파 조화 가속 검사, 외반고리관의 조직검사로 평가되었다. 청력검사 상 모든 *Slc26a4* 동형접합성 유전자결핍 마우스는 전농을 보인 반면, 형질변환 마우스, 이형접합성 마우스, 정상 대조군 마우스에서는 정상 청력을 나타내어 청각 기능의 all-or-none 표현형을 보였다. 정현파 조화 가속 검사에서는 동형접합성 마우스의 전정-안구 반사 반응이 거의 관찰되지 않았고, 형질변환 마우스와 이형접합성 마우스는 각각 동형접합체과 정상 대조군 사이의 중간 반응이 확인되었으며, 이는 전정 기능이상의 펜드린 양-의존적인(dose-dependent) 양상을 반영한다. 조직검사 상 동형접합성 마우스의 외반고리관 전정세포에서 액포 치환과

calretinin 발현 부재가 관찰되었으나, 형질변환 마우스, 이형접합체, 정상 마우스 간에는 내이 구조 상 유의미한 차이가 없었다. 이러한 결과들은 마우스 모델에서 *Slc26a4* 유전자의 돌연변이가 외반고리관의 다양한 기능적 결핍과 가변적인 징후가 동반되는 전정질환을 일으킬 수 있음을 시사한다.

주요어: 펜드린, *SLC26A4* 유전자, 전정-안구 반사, 외반고리관, 전정 질환, 전정수도관 확장증, 감각신경성 난청

학번: 2010-30525